



Effects of temperature dependence of thermoelectric properties on the power and efficiency of a multielement thermoelectric generator

Fankai Meng, Lingen Chen, Fengrui Sun

College of Naval Architecture and Power, Naval University of Engineering, Wuhan 430033, P. R. China.

Abstract

Taking temperature dependence of thermoelectric properties and external heat transfer irreversibility into account synchronously, an improved finite time thermodynamic model of a multi-element thermoelectric generator is established. The theoretical iterative functions of the hot and cold junction temperatures are obtained. The model is applied to the analysis of a multi-element thermoelectric generator, which is made of typical thermoelectric materials. The effects of output electrical current, length of thermoelectric element and ratio of thermal conductance allocation of heat exchangers on the power and efficiency are analyzed, along with the optimal variables. Comparing this temperature dependent model with the traditional temperature independent model, it is found that the temperature dependence of thermoelectric properties has significant effects on the power, efficiency and optimal variables. Specially, for a large temperature difference, the temperature independent model will cause a considerable error, so it is recommended to apply this temperature dependent model for the analysis of practical thermoelectric generator. Because of the effects of temperature dependence of thermoelectric properties, a limit of efficiency of about 7% can not be overrun. The model and calculation method provided in this paper may be applied to not only the calculation, prediction but also the design and optimization of thermoelectric generators.

Copyright © 2012 International Energy and Environment Foundation - All rights reserved.

Keywords: Thermoelectric generator; Temperature dependence; Energy recovery; Power; Efficiency.

1. Introduction

Thermoelectric generators [1] are solid-state energy converters, whose combination of thermal, electrical and semiconductor properties allows them to be used to convert waste heat into electricity or electrical power directly [2-5]. These devices can be competitive with fluid-based systems, such as two-phase air-conditioning compressors or heat pumps, or used in smaller-scale applications. In the last years, considerable efforts have been developed to identify new classes of thermoelectric materials [6-8] with enhanced performances. In addition to the improvement of the thermoelectric material and module, the system analysis and optimization of thermoelectric generators are equally important in designing high-performance thermoelectric generators [9, 10].

In general, conventional non-equilibrium thermodynamics [11-13] is used to analyze the performance of single-stage one or multiple-element thermoelectric generators. Considering the inner structure of a thermoelectric generator, a significant increase in the power output from a module can be achieved by modifying the geometry of the thermo-elements [14, 15]. Rowe [16, 17] investigated the efficiency of a

single couple solar powered thermoelectric generator and reviewed US applications of nuclear-powered thermoelectric generators in space. Chen *et al.* [18] investigated the influence of Thomson effect on the maximum power output and maximum efficiency of a thermoelectric generator. Yamashita [19] derived the resultant Seebeck coefficient of a thermoelectric element analytically from the temperature dependence of the intrinsic Seebeck coefficient by taking into account the Thomson effect.

Thermoelectric devices can not be used independently. They should be connected with heat exchangers to dissipate heat [2-5]. Considering the external irreversibilities of a thermoelectric generator, much work has shown that the heat transfer irreversibilities between the device and its external reservoirs affect the performances of thermodynamic processes strongly. The theory of finite time thermodynamics or entropy-generation minimization [20-26] is a powerful tool for the performance analysis and optimization of practical thermodynamic processes and devices, especially for finite rate heat transfer. Some authors have investigated the performances of thermoelectric generators using a combination of finite time thermodynamics and non-equilibrium thermodynamics. Gordon [27], Wu [28], Agrawal *et al.* [29], Chen *et al.* [30, 31] and Nuwayhid *et al.* [32] analyzed the effect of finite rate heat transfer between the thermoelectric device and its external heat reservoirs on the performance of single-element thermoelectric generators.

In practice, a commercial thermoelectric generator is a multielement device, which is composed of many fundamental thermoelectric elements. Many researchers investigated the characteristics of multielement thermoelectric generators with the irreversibility of external finite-rate heat transfer, Joulean heat inside the thermoelectric device, and the heat leakage through the thermoelectric element. Chen *et al.* [33, 34] analyzed the effects of external heat conductance and the number of elements on the power output and efficiency of a multi-elements generator. Yu and Zhao [35] presented a numerical model to predict the performance of thermoelectric generator with the parallel-plate heat exchanger. Niu *et al.* [36] constructed an experimental thermoelectric generator unit incorporating the commercially available thermoelectric modules with the parallel-plate heat exchanger. Hsiao *et al.* [37] built a one dimensional thermal resistance model to predict the behavior of thermoelectric modules applied in exhaust and radiator of an automobile. Chen [38], Khattab and Shenawy [39], and Meng *et al.* [40-43] investigated the feasibility and performance optimization of a single (two) stage thermoelectric refrigerator or heat pump driven by a single (two) stage thermoelectric generator. There is no research concerning thermoelectric generator considering external heat transfer and temperature dependence of thermoelectric properties synchronously in open literatures.

Taking temperature dependence of thermoelectric properties and external heat transfer irreversibilities into account synchronously, a finite time thermodynamic model of multielement thermoelectric generator is established in this paper, based on which, the power and efficiency of a practical multielement thermoelectric generator are calculated at different temperature difference. The effects of output electrical current, length of thermoelectric element and ratio of thermal conductance allocation of the heat exchangers on the power and efficiency are analyzed, along with the optimal variables.

2. System modeling and energy equations

A multielement thermoelectric generator with external heat transfer is shown in Figure 1. A thermoelectric generator consists of P-type and N-type semiconductor legs. A P-type and an N-type semiconductor leg compose a thermoelectric element. The geometry structure of a thermoelectric element is shown in Figure 2. The length and cross section area of a thermoelectric semiconductor leg are L and A . The number of thermoelectric elements is N . The junctions of the thermoelectric elements are fixed at a thermal conducting and electrical insulating ceramic plate. The area of the ceramic plate is A_m . The module packed density θ is defined as $\theta = 2AN / A_m$ [15].

The hot and cold junction temperatures are T_h and T_c . The heat source and heat sink temperatures are T_H and T_L . The heat flow rate absorbed from the heat source of the thermoelectric generator is Q_H . The heat flow rate dissipated from the thermoelectric generator to the heat sink is Q_L . The heat flow rate through the hot and cold junctions of the thermoelectric elements are Q_h and Q_c . It is assumed that the heat transfers between the heat reservoirs and the thermoelectric generator are finite rate irreversible heat transfer and obey Newtonian heat transfer law $Q \propto \Delta T$.

The electrical resistance of the P- and N- type semiconductor leg are R_p and R_n . The output electrical current and load resistance are I and R_L .

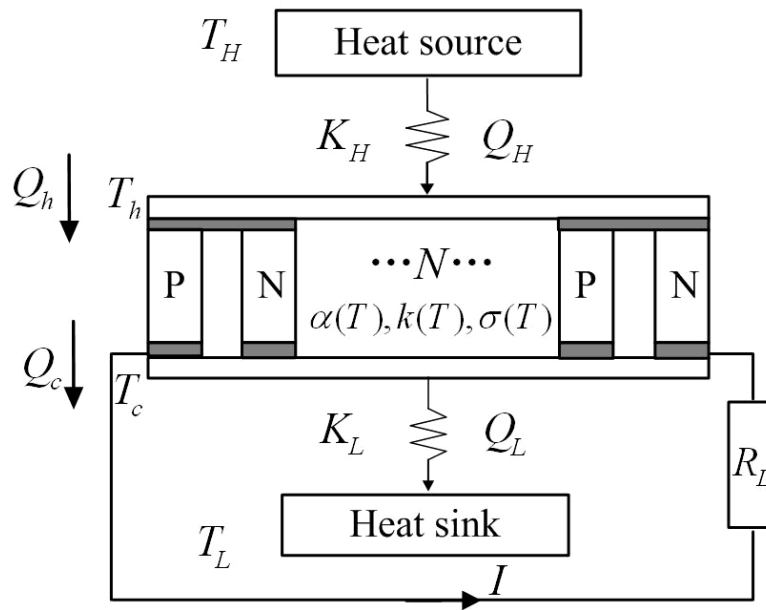


Figure 1. Schematic diagram of a multielement thermoelectric generator with external heat

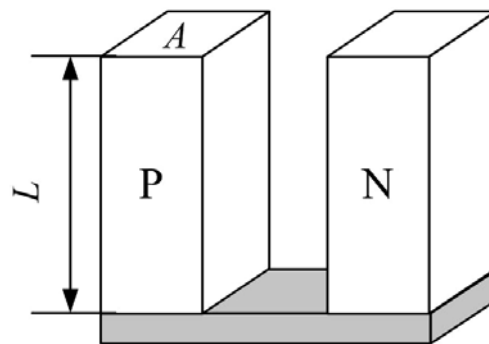


Figure 2. The geometry structure of a thermoelectric element

For a well design thermal insulation packaging module, the heat leakage from the surrounding of the elements and module can be neglected, so the heat transfer of the whole device can be treated as one dimensional heat transfer. According to the non-equilibrium thermodynamics, the inner effects of the thermoelectric elements include Seebeck effect, Fourier effect, Joule effect and Thomson effect. The increment rate of inner energy of the infinitesimal is zero at steady-state. One can obtain the heat conduction differential equations of P- and N-Type semiconductor legs as follows [1]

$$k_p A_p \frac{dT_p^2}{dx^2} + \mu_p I \frac{dT_p}{dx} + \frac{I^2}{\sigma_p A_p} = 0 \quad (1)$$

$$k_n A_n \frac{dT_n^2}{dx^2} - \mu_n I \frac{dT_n}{dx} + \frac{I^2}{\sigma_n A_n} = 0 \quad (2)$$

where k_p , σ_p , μ_p , A_p , L_p , T_p and k_n , σ_n , μ_n , A_n , L_n , T_n are the thermal conductivity, electrical conductivity, Thomson coefficient, cross section area, length and temperature of the P-type and N-type semiconductor leg, respectively.

The temperature boundary conditions are;

$$T_p(0) = T_n(0) = T_c \quad (3)$$

$$T_p(L_p) = T_n(L_n) = T_h \tag{4}$$

Taking effect of temperature dependence of thermoelectric properties into account, k_p , σ_p and μ_p are functions of T_p ; while k_n , σ_n and μ_n are functions of T_n . However, such a differential equation can not be solved theoretically. Replacing k , σ and μ with the mean value \bar{k} , $\bar{\sigma}$ and $\bar{\mu}$ approximately gives approximations of Eqs. (1) and (2) as follows;

$$\bar{k}_p A_p \frac{dT_p^2}{dx^2} + \bar{\mu}_p I \frac{dT_p}{dx} + \frac{I^2}{\bar{\sigma}_p A_p} = 0 \tag{5}$$

$$\bar{k}_n A_n \frac{dT_n^2}{dx^2} - \bar{\mu}_n I \frac{dT_n}{dx} + \frac{I^2}{\bar{\sigma}_n A_n} = 0 \tag{6}$$

where $\bar{k}_p \approx k_p|_{T=(T_h+T_c)/2}$, $\bar{\sigma}_p \approx \sigma_p|_{T=(T_h+T_c)/2}$, and $\bar{\mu}_p \approx \mu_p|_{T=(T_h+T_c)/2}$ for P-type semiconductor leg and for N-type likewise. The total heat flow rates through the hot and cold junctions are;

$$Q_h = N \left((\alpha_{ph} - \alpha_{nh}) T_h I + \bar{k}_p A_p \left. \frac{dT_p}{dx} \right|_{x=L_p} + \bar{k}_n A_n \left. \frac{dT_n}{dx} \right|_{x=L_n} \right) \tag{7}$$

$$Q_c = N \left((\alpha_{pc} - \alpha_{nc}) T_c I + \bar{k}_p A_p \left. \frac{dT_p}{dx} \right|_{x=0} + \bar{k}_n A_n \left. \frac{dT_n}{dx} \right|_{x=0} \right) \tag{8}$$

where α_p and α_n are the Seebeck coefficients of the P- and N- type semiconductor leg, and the subscripts h and c represent the hot and cold sides.

It is assumed that the external thermal conductances at hot and cold sides are K_H and K_L , respectively. Then one has;

$$Q_H = K_H (T_H - T_h) \tag{9}$$

$$Q_L = K_L (T_c - T_L) \tag{10}$$

The heat flow balance equations are;

$$Q_H = Q_h \tag{11}$$

$$Q_L = Q_c \tag{12}$$

3. Solution of the model

The temperature distributions of the P- and N- type semiconductor legs can be solved by Eqs. (5) and (6) as follows;

$$T_p(x) = T_c - F_p x + \frac{T_h - T_c + F_p L_p}{(e^{-\omega_p L_p} - 1)} (e^{-\omega_p x} - 1) \tag{13}$$

$$T_n(x) = T_c + F_n x + \frac{T_h - T_c - F_n L_n}{(e^{\omega_n L_n} - 1)} (e^{\omega_n x} - 1) \tag{14}$$

where $\omega_p = \bar{\mu}_p I / (\bar{k}_p A_p)$, $F_p = I / (\bar{\sigma}_p \bar{\mu}_p A)$, $\omega_n = \bar{\mu}_n I / (\bar{k}_n A_n)$ and $F_n = I / (\bar{\sigma}_n \bar{\mu}_n A)$.

For maximum figure of merit of the thermoelectric element $Z = \alpha^2 / (KR)$, the physical dimension of the thermoelectric element and the physical property of the material should satisfy the following equation [1, 2].

$$\frac{A_p^2 L_n^2}{A_n^2 L_p^2} = \frac{k_n \sigma_n}{k_p \sigma_p} \quad (15)$$

To reduce the cost of manufacture, the P- and N- type semiconductor legs are made with same physical dimensions in general, i.e. $A_p = A_n = A$ and $L_p = L_n = L$. So one has $k_n \sigma_n / (k_p \sigma_p) = 1$ by Eq. (15). Similar doped alloys are adopted to make P- and N- type semiconductor legs. That is, $\sigma_p = \sigma_n = \sigma$, $k_p = k_n = k$, $\alpha_p = -\alpha_n$, and $\mu_p = -\mu_n$. According to Taylor's expansion formula, when $|x| \ll 1$, $e^x \approx 1 + x$ holds truly. Based on the assumptions mentioned above, Eqs. (7) and (8) can be approximated as follows in the case of $\bar{\mu}l / K \ll 1$:

$$Q_h = N[\alpha_h IT_h + K(T_h - T_c) - 0.5I^2R - 0.5\bar{\mu}l(T_h - T_c)] \quad (16)$$

$$Q_c = N[\alpha_c IT_c + K(T_h - T_c) + 0.5I^2R + 0.5\bar{\mu}l(T_h - T_c)] \quad (17)$$

where $\alpha_h = \alpha_{hp} - \alpha_{hn}$ and $\alpha_c = \alpha_{cp} - \alpha_{cn}$ are the Seebeck coefficients of the thermoelectric elements at hot and cold sides. $\bar{\mu} = \bar{\mu}_p - \bar{\mu}_n = 2\bar{\mu}_p$, K and R are the total Thomson coefficient, thermal conductance and electrical resistance of a thermoelectric element. αIT , $K\Delta T$, I^2R and $\bar{\mu}l\Delta T$ are the rates of Peltier heat, Fourier heat, Joule heat and Thomson heat, respectively. K and R are given by;

$$K = K_p + K_n = \bar{k}_p A_p / L_p + \bar{k}_n A_n / L_n = 2\bar{k}A / L \quad (18)$$

$$R = R_p + R_n = L_p / (\bar{\sigma}_p A_p) + L_n / (\bar{\sigma}_n A_n) = 2L / (\bar{\sigma}A) \quad (19)$$

The output power is given by;

$$P = Q_h - Q_c = NI[\alpha_h T_h - \alpha_c T_c - IR - \bar{\mu}l(T_h - T_c)] \quad (20)$$

The contact resistance is also considered in this paper. The contact resistance is in proportion to the reciprocal of the contact area with same manufacture and same thickness of the contact zone [1]. That is, $R_{ct} = C_{ct} / A$, where C_{ct} is a constant independent of the length of the thermoelectric element and A is the cross area of a semiconductor leg.

Taking the Joule heat generated by the contact resistance as the thermoelectric elements generated and replacing R with $R_t = R + R_{ct}$ give the modified output power as follows;

$$P = Q_h - Q_c = NI[\alpha_h T_h - \alpha_c T_c - IR_t - \bar{\mu}l(T_h - T_c)] \quad (21)$$

The efficiency $\eta = P / Q_H$ is given by;

$$\eta = \frac{NI[\alpha_h T_h - \alpha_c T_c - IR_t - \bar{\mu}l(T_h - T_c)]}{N[\alpha_h IT_h + K(T_h - T_c) - 0.5I^2R_t - 0.5\bar{\mu}l(T_h - T_c)]} \quad (22)$$

Note that not only the temperature dependence of thermoelectric properties but also the external heat transfer is considered in this paper. For given heat source and heat sink temperatures T_H and T_L , the junction temperatures of thermoelectric element T_h and T_c are unknown, thus the thermoelectric properties α_h , α_c , \bar{k} and $\bar{\sigma}$ and $\bar{\mu}$ are unknown. Alteration method is adopted herein to determine the

junction temperatures T_h and T_c . The alteration formula can be solved by Eqs. (11) and (12) as follows;

$$T_h = \frac{N^2 R_i \alpha_c I^3 + (-2N^2 R_i K - N R_i K_L) I^2 + [2N \alpha_c K_H T_H + (N K_L T_L - K_H T_H N) \bar{\mu}] I - 2K_H T_H N K - 2N K K_L T_L - 2K_L K_H T_H}{[2N^2 \alpha_h \alpha_c - (N^2 \alpha_c + N^2 \alpha_h) \bar{\mu}] I^2 - [2N^2 \alpha_h K + (K_H N - N K_L) \bar{\mu} - 2K_H N \alpha_c + 2N \alpha_h K_L - 2N^2 K \alpha_c] I - 2K_H N K - 2N K K_L - 2K_H K_L} \quad (23)$$

$$T_c = \frac{N^2 \alpha_h I^3 R_i + (2N^2 R_i K + K_H N R_i) I^2 + [(-N K_L T_L + K_H T_H N) \bar{\mu} + 2N \alpha_h K_L T_L] I + 2K_H T_H N K + 2K_H K_L T_L + 2N K K_L T_L}{[-2N^2 \alpha_h \alpha_c + (N^2 \alpha_c + N^2 \alpha_h) \bar{\mu}] I^2 + [2N^2 \alpha_h K + (K_H N - N K_L) \bar{\mu} - 2K_H N \alpha_c + 2N \alpha_h K_L - 2N^2 K \alpha_c] I + 2K_H N K + 2N K K_L + 2K_H K_L} \quad (24)$$

where α_h , α_c , K , R_i and $\bar{\mu}$ are functions of T_h and T_c . For given initial values of T_h and T_c ($T_h = T_H, T_c = T_L$, for example), α_h , α_c , K , R_i and $\bar{\mu}$ can be calculated by the fitting equation of the thermoelectric material. Then T_h and T_c can be calculated by Eqs. (23) and (24). Repeating the process until required precision is obtained.

If the temperature dependence of thermoelectric properties is not considered, the model changes into a temperature independent model, and then Eqs.(16) and (17) change into;

$$Q_h = N[\alpha I T_h + K(T_h - T_c) - 0.5I^2 R] \quad (25)$$

$$Q_c = N[\alpha I T_c + K(T_h - T_c) + 0.5I^2 R] \quad (26)$$

Eqs. (23) and (24) change into [27, 28, 31, 33, 34, 37].

$$T_h = \frac{0.5N^2 R_i \alpha I^3 + (-N^2 R_i K - 0.5N R_i K_L) I^2 + N \alpha K_H T_H I - N K (K_H T_H + K_L T_L) - K_L K_H T_H}{N^2 \alpha^2 I^2 + N \alpha (K_H - K_L) I - N K (K_H + K_L) - K_H K_L} \quad (27)$$

$$T_c = \frac{0.5N^2 \alpha I^3 R_i + (N^2 R_i K + 0.5N R_i K_H) I^2 + N \alpha K_L T_L I + N K (K_H T_H + K_L T_L) + K_H K_L T_L}{-N^2 \alpha^2 I^2 + N \alpha (K_L - K_H) I + N K (K_H + K_L) + K_H K_L} \quad (28)$$

The junction temperatures T_h and T_c can be solved analytically herein.

4. Effects of temperature dependence of thermoelectric properties

When the external heat transfer is considered, the allocation of thermal conductance of heat exchangers between the hot and cold sides affects the performance of the thermoelectric devices [33, 34]. To describe the allocation, a ratio of thermal conductance allocation is defined as $f = K_H / (K_H + K_L)$.

The characteristics of power and efficiency versus output electrical current, length of thermoelectric element and ratio of thermal conductance allocation are investigated by numerical calculations. The physical properties of the commercially available material by Melcor [44] used for this simulation are shown as follows;

$$\alpha_p = (22224.0 + 930.6T - 0.9905T^2)10^{-9} \text{ V/K} \quad (29)$$

$$\rho = (5112.0 + 163.4T + 0.6279T^2)10^{-10} \text{ } \Omega\text{m} \quad (30)$$

$$k = (62605.0 - 277.7T + 0.4131T^2)10^{-4} \text{ W/m/K} \quad (31)$$

where α_p , ρ and k are the Seebeck coefficient, electrical resistivity and thermal conductivity. The Thomson coefficient is given by the second Kelvin relationship [1];

$$\mu = T \frac{d\alpha}{dT} \quad (32)$$

Two models, i.e. the temperature dependent model established in this paper and the traditional temperature independent model will be analyzed, optimized and compared with each other in this section. The thermoelectric properties of the temperature independent model (at $T = 300\text{K}$) and base-line parameters of the two models are listed in Table 1. The optimal variables at maximum power and the corresponding maximum powers of the two models are listed in Table 2. The optimal variables at maximum efficiency and the corresponding maximum efficiencies of the two models are listed in Table 3. The superscript T denotes that the temperature dependence of thermoelectric properties is considered in the optimization, i.e. the results of the temperature dependent model.

Figures 3 and 4 show the effects of temperature dependence on the characteristics of power P and efficiency η versus electrical current I . The results of temperature independent and dependent models are displayed by dotted and solid lines, respectively. The results at $\Delta T = 150\text{K}$ and at $\Delta T = 250\text{K}$ are displayed by circle and square markers, respectively. $L = 1\text{mm}$ and $f = 0.5$ are set in the figures. It can be seen that the shapes of curves of the two models are similar, i.e. parabola-like. There is one optimal electrical current I^P corresponding to the maximum power and another optimal electrical current I^η corresponding to the maximum efficiency. $P^T > P$ at $\Delta T = 150\text{K}$ while $P^T < P$ at $\Delta T = 250\text{K}$. The results of optimization of electrical current show that for maximum power or for maximum efficiency, when the temperature difference is small ($\Delta T < 200\text{K}$), $I_o^T > I_o$ and $P_{\max}^T > P_{\max}$ holds (see Table 2); when the temperature difference is large ($\Delta T > 200\text{K}$), $I_o^T < I_o$ and $P_{\max}^T < P_{\max}$ holds (see Table 3).

Figures 5 and 6 show the effects of temperature dependence on the characteristics of power P and efficiency η versus length of thermoelectric element L . $I = 0.5\text{A}$ and $f = 0.5$ are set in the figures. One can see that the shapes of curves of the two models are similar, i.e. increase rapidly at the start and decrease slowly after the maximum. There is one optimal length of thermoelectric element L^P corresponding to the maximum power and another optimal length of thermoelectric element L^η corresponding to the maximum efficiency. The zero-power length of thermoelectric element $L_{P=0}^T < L_{P=0}$. The results of optimization of length of thermoelectric element show that for maximum power, $L_o^T < L_o$ holds. When $\Delta T < 250\text{K}$, $P_{\max}^T > P_{\max}$ holds; when $\Delta T > 250\text{K}$, $P_{\max}^T < P_{\max}$ holds (see Table 2). For maximum efficiency, $L_o^T < L_o$ holds in general. When $\Delta T < 150\text{K}$, $P_{\max}^T > P_{\max}$ holds; when $\Delta T > 150\text{K}$, $P_{\max}^T < P_{\max}$ holds (see Table 3).

Figures 7 and 8 show the effects of temperature dependence on the characteristics of power P and efficiency η versus ratio of thermal conductance allocation f . $I = 0.5\text{A}$ and $L = 1\text{mm}$ are set in the figures. One can see that the shapes of curves of the two models are similar, i.e. smooth in a wide range but decrease rapidly when f near 0 or 1. There is one optimal ratio of thermal conductance allocation f^P and another optimal ratio f^η corresponding to the maximum power and maximum efficiency, respectively. The results of optimization of ratio of thermal conductance allocation show that for maximum power, $f_o^T > f_o \equiv 0.5$ holds. When $\Delta T < 250\text{K}$, $P_{\max}^T > P_{\max}$ holds; when $\Delta T > 200\text{K}$, $P_{\max}^T < P_{\max}$ (see Table 2). For the maximum efficiency, $f_o^T > f_o$ holds in general. When $\Delta T < 200\text{K}$, $P_{\max}^T > P_{\max}$ holds; when $\Delta T > 200\text{K}$, $P_{\max}^T < P_{\max}$ holds (see Table 3).

To sum up, if the temperature dependence of thermoelectric properties is not considered, increasing the

temperature difference will always improve the power and efficiency. However, because of the effects of temperature dependence of thermoelectric properties, with the increase of temperature difference, the power improves more and more slowly while the efficiency decreases after its maximum. In this case, a limit of 7% for efficiency can not be overrun.

Comparing the optimal variables in Table 1 with those in Table 2, some relations can be concluded as follows;

$$I_o^P > I_o^\eta \tag{33}$$

$$L_o^P < L_o^\eta \tag{34}$$

$$f_o^P < f_o^\eta \tag{35}$$

where the superscript P and η denote at maximum power and at maximum efficiency. Eqs. (33)-(35) give the basic principles of optimal variables section.

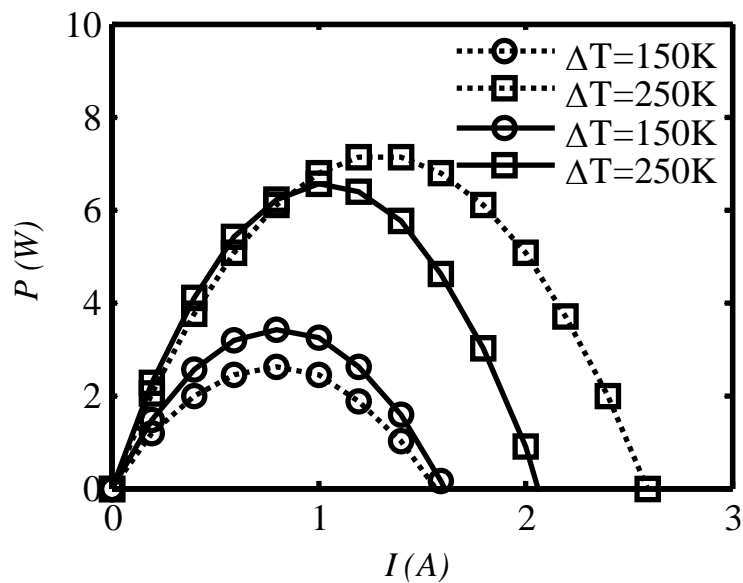


Figure 3. Effects of temperature dependence on power versus electrical current

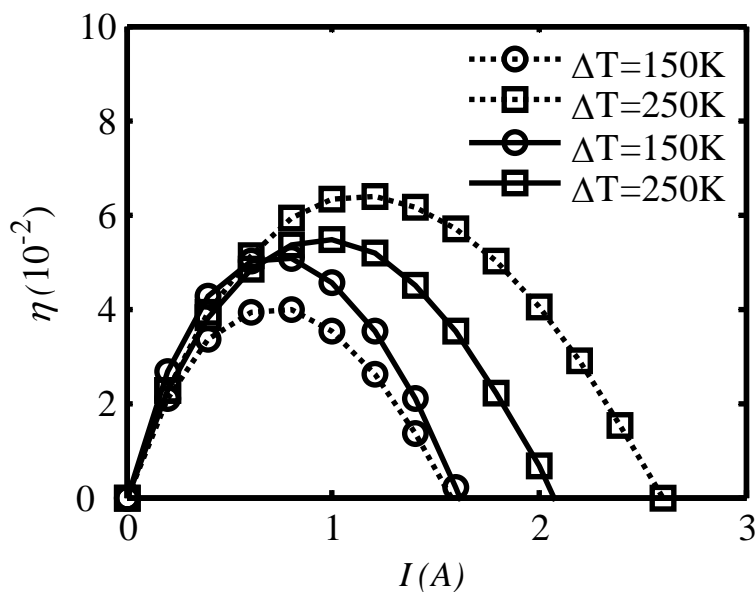


Figure 4. Effects of temperature dependence on efficiency versus electrical current

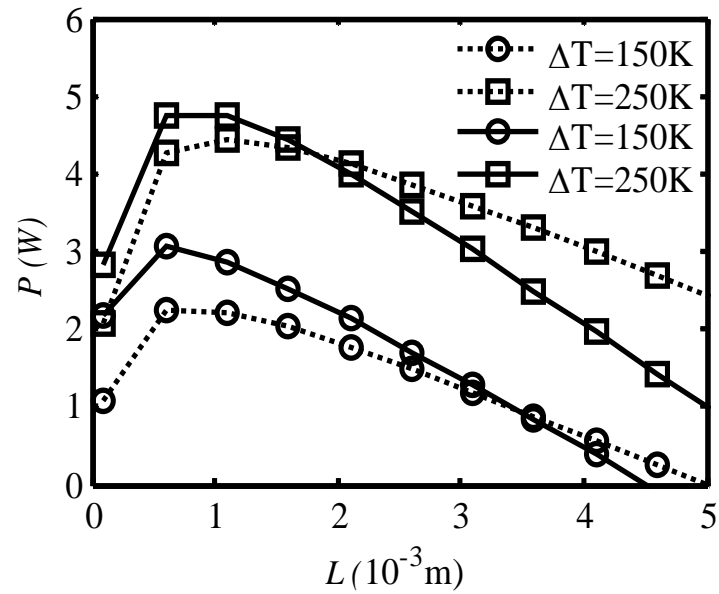


Figure 5. Effects of temperature dependence on power versus length of thermoelectric element

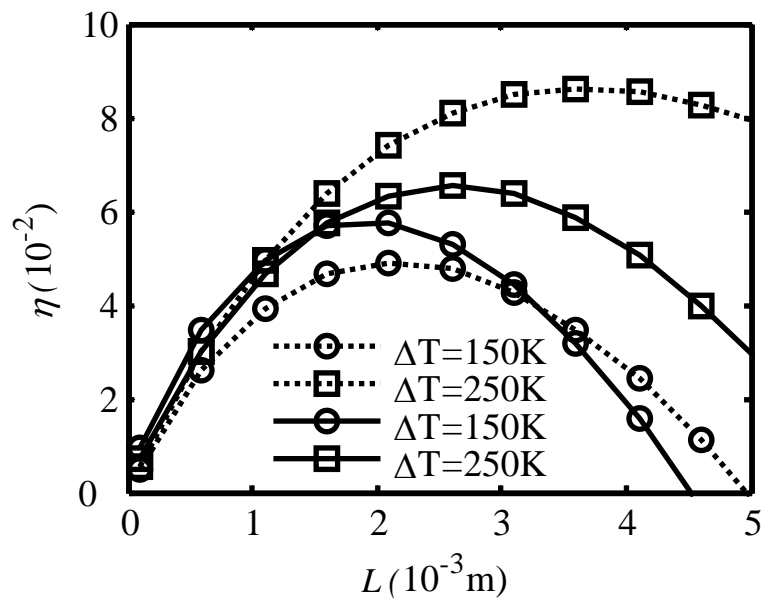


Figure 6. Effects of temperature dependence on efficiency versus length of thermoelectric element

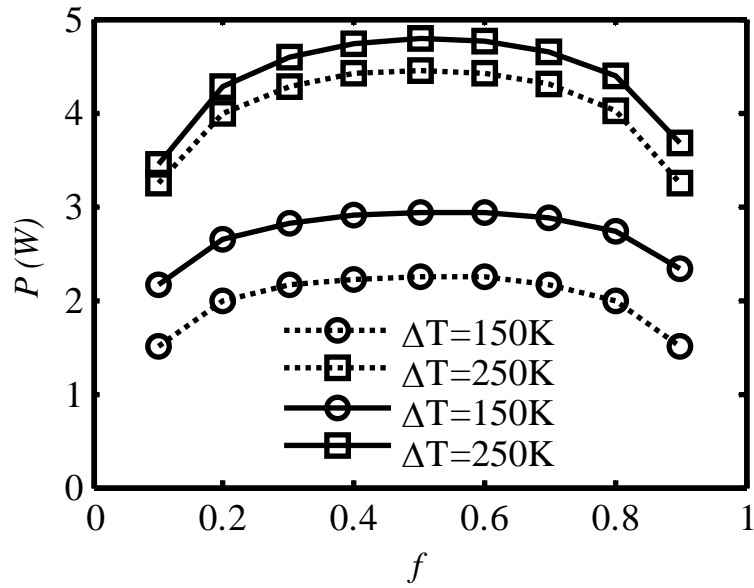


Figure 7. Effects of temperature dependence on power versus ratio of thermal conductance allocation

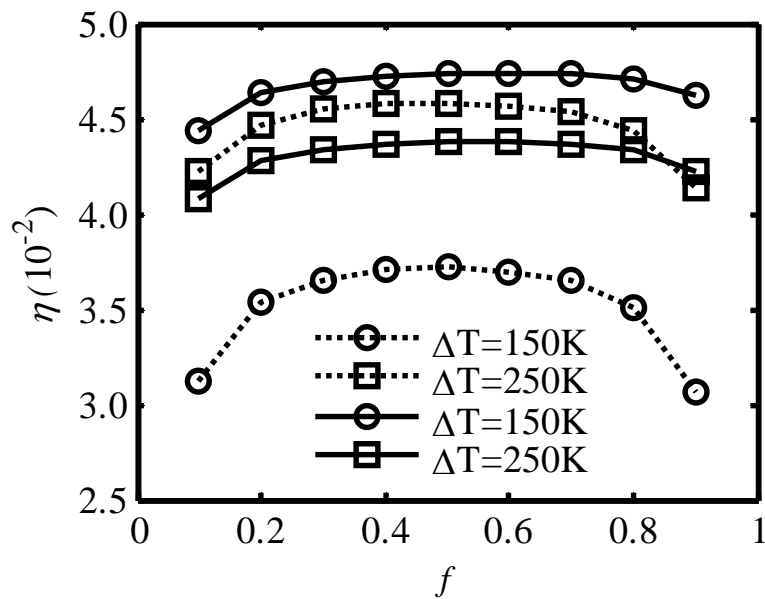


Figure 8. Effects of temperature dependence on efficiency versus ratio of thermal conductance allocation

Table 1 Base-line case parameters

$\alpha(VK^{-1})$	$\sigma(\Omega^{-1}m^{-1})$	$k(Wm^{-1}K^{-1})$	$A_m(mm^2)$	$A(mm^2)$	θ	N	$C_{gr}(\Omega m^2)$	$I_L(K)$	$K_T(WK^{-1})$	$I(A)$	$L(mm)$	f
4.25×10^{-4}	9.04×10^4	1.65	20×20	1	0.6	120	10^{-8}	300	10	0.5	1	0.5

Table 2 The optimal variables at maximum power and the corresponding maximum powers of the two models

$\Delta T(K)$	$I_o(A)$	$I_o^I(A)$	$P_{max}(W)$	$P_{max}^I(W)$	$L_o(mm)$	$L_o^I(mm)$	$P_{max}(W)$	$P_{max}^I(W)$	f_o	f_o^I	$P_{max}(W)$	$P_{max}^I(W)$
100	0.55	0.60	1.16	1.74	0.60	0.46	1.25	1.89	0.50	0.52	1.16	1.69
150	0.80	0.80	2.60	3.42	0.78	0.60	2.28	3.05	0.50	0.53	2.25	2.93
200	1.05	0.95	4.59	5.15	0.94	0.70	3.35	4.06	0.50	0.53	3.35	3.99
250	1.30	1.05	7.14	6.53	1.06	0.80	4.44	4.82	0.50	0.52	4.44	4.79
300	1.55	1.05	10.22	7.26	1.18	0.90	5.55	5.27	0.50	0.51	5.53	5.26

Table 3 The optimal variables at maximum efficiency and the corresponding maximum efficiencies of the two models

$\Delta T(K)$	$I_o(A)$	$I_o^I(A)$	$\eta_{max}(10^{-2})$	$\eta_{max}^I(10^{-2})$	$L_o(mm)$	$L_o^I(mm)$	$\eta_{max}(10^{-2})$	$\eta_{max}^I(10^{-2})$	f_o	f_o^I	$\eta_{max}(10^{-2})$	$\eta_{max}^I(10^{-2})$
100	0.50	0.55	2.73	3.99	1.34	1.36	2.89	4.20	0.50	0.54	2.73	3.99
150	0.70	0.70	4.01	5.13	2.14	1.92	4.91	5.79	0.49	0.59	3.72	4.74
200	0.95	0.85	5.22	5.60	2.92	2.32	6.82	6.53	0.48	0.60	4.25	4.76
250	1.15	0.95	6.38	5.45	3.68	2.60	8.63	6.53	0.48	0.56	4.58	4.38
300	1.35	1.00	7.50	4.81	4.42	2.74	10.34	5.92	0.47	0.51	4.81	3.76

8. Conclusion

Taking temperature dependence of thermoelectric properties and external heat transfer irreversibilities into account, a new model of multielement thermoelectric generator is established. Applying the model to a practical multielement generator, it is found that the temperature dependence of thermoelectric properties has a significant effect on the power, efficiency and optimal variables. If the temperature dependence of thermoelectric properties is not considered, increasing the temperature difference will always improve the power and efficiency. However, because of the effects of temperature dependence of thermoelectric properties, with the increase of temperature difference, the power improves more and more slowly while the efficiency decreases after its maximum. Specially, when the temperature difference is large, the temperature independent model will cause a considerable error, so it is recommended to apply this temperature dependent model for the calculations of practical multielement thermoelectric generators. The model and calculation method provided in this paper may be applied to not only the calculation, prediction but also design and optimization for thermoelectric generators.

Acknowledgements

This paper is supported by the National Natural Science Foundation of P. R. China (Project No. 10905093) and the Natural Science Foundation of Naval University of Engineering (HGDYDJJ10011). The authors wish to thank the reviewers for their careful, unbiased and constructive suggestions, which led to this revised manuscript.

Nomenclature

A	Area (m^2)
C	Coefficient
f	Ratio of thermal conductance allocation
I	Output electrical current (A)
K	Thermal conductance (WK^{-1})
k	Thermal conductivity ($Wm^{-1}K^{-1}$)
L	Length (m)
N	Number
P	Output power (W)
Q	Heat flow rate (W)
R	Electrical resistance (Ω)
T	Temperature (K)

Greek letters

α	Seebeck coefficient (VK^{-1})
Δ	Difference
δ	Thickness (m)
η	Thermal efficiency
μ	Thomson coefficient (VK^{-2})

θ	Packed density
ρ	Electrical resistivity (Ωm)
σ	Electrical conductivity ($\Omega^{-1}m^{-1}$)

Subscripts

c	Cold junction
ct	Contact
H	Heat source
h	Hot junction
n	N-type semiconductor leg
o	Optimal
p	P-type semiconductor leg
T	Total

Superscripts

P	At maximum output power
T	Temperature dependent
η	At maximum efficiency

References

- [1] Ioffe A F. Semiconductor Thermoelements and Thermoelectric Cooling. London: Infosearch, 1957.
- [2] Blatt J. Thermoelectric Power of Metals. New York: Springer, 1976.
- [3] Kutasov V A. Thermoelectric Properties of Semiconductors. New York: Consultants Bureau, 1964.
- [4] Riffat S B, Ma X. Thermoelectrics: a review of present and potential applications. Appl. Thermal Engng., 2003, 23(8): 913-935.
- [5] Rowe D M. Thermoelectrics Handbook: Macro to Nano. Boca Raton: CRC Press, 2005.
- [6] Ahmed M A, Okasha N, Kershi R M. Extraordinary role of rare-earth elements on the transport properties of barium W-type hexaferrite. Mater. Chem. Phys., 2009, 113(1): 196-201.
- [7] Fayek M K, Ata-Allah S S, Roumah K, Ismail S. Thermoelectric power properties of Zn substituted Cu-Ga spinel ferrites. Materials Letters, 2009, 63(12): 1010-1012.

- [8] Patil N S, Sargar A M, Mane S R, Bhosale P N. Effect of Sb doping on thermoelectric properties of chemically deposited bismuth selenide films. *Mater. Chem. Phys.*, 2009, 115(1): 47-51.
- [9] Thomas J P, Qidwai M A, Kellogg J C. Energy scavenging for small-scale unmanned systems. *J. Power Sources*, 2006, 159(2): 1494-1509.
- [10] Hosono H. *Nanomaterials: From Research to Applications*. Amsterdam: Elsevier, 2006.
- [11] Angrist S W. *Direct Energy Conversion (4th Ed)*. Boston: Allyn and Bacon, 1992.
- [12] Radcenco V. *Generalized Thermodynamics*. Bucharest: Editura Tehnica, 1994.
- [13] Bejan A. *Advanced Engineering Thermodynamics (3rd Ed)*. Hoboken, N.J.: John Wiley & Sons, 2006.
- [14] Min G, Rowe D M. Optimisation of thermoelectric module geometry for 'waste heat' electric power generation. *J. Power Sources*, 1992, 38(3): 253-259.
- [15] Rowe D M, Min G. Evaluation of thermoelectric modules for power generation. *J. Power Sources*, 1998, 73(2): 193-198.
- [16] Rowe D M. A high performance solar powered thermoelectric generator. *Appl. Energy*, 1981, 8(4): 269-273.
- [17] Rowe D M. Applications of nuclear-powered thermoelectric generators in space. *Appl. Energy*, 1991, 40(4): 241-271.
- [18] Chen J, Yan Z, Wu L. The influence of Thomson effect on the maximum power output and maximum efficiency of a thermoelectric generator. *J. Appl. Phys.*, 1996, 79(11): 8823-8828.
- [19] Yamashita O. Resultant Seebeck coefficient formulated by combining the Thomson effect with the intrinsic Seebeck coefficient of a thermoelectric element. *Energy Convers. Mgnt.*, 2009, 50(9): 2394-2399.
- [20] Sieniutycz S, Salamon P. *Advances in Thermodynamics. Volume 4: Finite Time Thermodynamics and Thermoeconomics*. New York: Taylor & Francis, 1990.
- [21] de Vos A. *Endoreversible Thermodynamics of Solar Energy Conversion*. Oxford: Oxford University, 1992.
- [22] Bejan A. Entropy generation minimization: The new thermodynamics of finite-size devices and finite-time processes. *J. Appl. Phys.*, 1996, 79(3): 1191-1218.
- [23] Berry R S, Kazakov V A, Sieniutycz S, Szewast Z, Tsirlin A M. *Thermodynamic Optimization of Finite Time Processes*. Chichester: Wiley, 1999.
- [24] Gordon J M, Ng K C. *Cool Thermodynamics*. Cambridge: Cambridge Int. Science Publishers, 2000.
- [25] Chen L, Sun F. *Advances in Finite Time Thermodynamics: Analysis and Optimization*. New York: Nova Science Publishers, 2004.
- [26] Sieniutycz S, Jezowski J. *Energy Optimization in Process Systems*. Oxford: Elsevier, 2009.
- [27] Gordon J M. Generalized power versus efficiency characteristics of heat engines: the thermoelectric generator as an instructive illustration. *Am. J. Phys.*, 1991, 59(6): 551-555.
- [28] Wu C. Analysis of waste-heat thermoelectric power generators. *Appl. thermal Engng.*, 1996, 16(1): 63-69.
- [29] Agrawal D C, Menon V J. The thermoelectric generator as an endoreversible Carnot engine. *J. Phys. D: Appl. Phys.*, 1997, 30(2): 357-359.
- [30] Chen J, Andresen B. New bounds on the performance parameters of a thermoelectric generator. *Int. J. Power Energy Syst.*, 1997, 17(1): 23-27.
- [31] Chen J, Wu C. Analysis on the performance of a thermoelectric generator. *Trans. ASME J. Energy Res. Tech.*, 2000, 122(2): 61-63.
- [32] Nuwayhid R Y, Moukalled F. Evolution of power and entropy in a temperature gap system with electric and thermoelectric influences. *Energy Convers. Mgnt.*, 2003, 44(5): 647-665.
- [33] Chen L, Gong J, Sun F, Wu C. Effect of heat transfer on the performance of thermoelectric generators. *Int. J. thermal Sci.*, 2002, 41(1): 95-99.
- [34] Chen L, Sun F, Wu C. Heat transfer surface area optimization for a thermoelectric generator. *Int. J. Ambient Energy*, 2007, 28(3): 135-142.
- [35] Yu J, Zhao H. A numerical model for thermoelectric generator with the parallel-plate heat exchanger. *J. Power Sources*, 2007, 172(1): 428-434.
- [36] Niu X, Yu J, Wang S. Experimental study on low-temperature waste heat thermoelectric generator. *J. Power Sources*, 2009, 188(2): 621-626.

- [37] Hsiao Y Y, Chang W C, Chen S L. A mathematic model of thermoelectric module with applications on waste heat recovery from automobile engine. *Energy, The Int. J.*, 2010, 35(3): 1447-1454.
- [38] Chen X, Lin B, Chen J. The parametric optimum design of a new combined system of semiconductor thermoelectric devices. *Appl. Energy*, 2006, 83(7): 681-686.
- [39] Khattab N M, Shenawy E T E. Optimal operation of thermoelectric cooler driven by solar thermoelectric generator. *Energy Convers. Mgnt.*, 2006, 47(4): 407-426.
- [40] Meng F, Chen L, Sun F. Performance optimization for two-stage thermoelectric refrigerator system driven by two-stage thermoelectric generator. *Cryogenics*, 2009, 49(2): 57-65.
- [41] Chen L, Meng F, Sun F. A novel configuration and performance for a two-stage thermoelectric heat pump system driven by a two-stage thermoelectric generator. *Proc. IMechE, Part A, J. Power Energy*, 2009, 223(A4): 329-339.
- [42] Chen L, Meng F, Sun F. Effect of heat transfer on the performance of a thermoelectric heat pump driven by a thermoelectric generator. *Rev. Mex. Fis.*, 2009, 55(4): 282-291.
- [43] Meng F, Chen L, Sun F. Extreme working temperature differences for thermoelectric refrigerating and heat pumping devices driven by thermoelectric generator. *J. Energy Inst.*, 2010, 83(2): 108-113.
- [44] <<http://www.melcor.com>> homepage of Melcor, USA, 2009.



Fankai Meng received all his degrees (BS, 2005; MS, 2007, PhD, 2011) in power engineering and engineering thermophysics from the Naval University of Engineering, P R China. His work covers topics in finite time thermodynamics and technology support for thermoelectric devices. Dr Meng is the author or co-author of over 20 peer-refereed articles (12 in English journals).



Linggen Chen received all his degrees (BS, 1983; MS, 1986, PhD, 1998) in power engineering and engineering thermophysics from the Naval University of Engineering, P R China. His work covers a diversity of topics in engineering thermodynamics, constructal theory, turbomachinery, reliability engineering, and technology support for propulsion plants. He had been the Director of the Department of Nuclear Energy Science and Engineering, the Director of the Department of Power Engineering and the Superintendent of the Postgraduate School. Now, he is the Dean of the College of Naval Architecture and Power, Naval University of Engineering, P R China. Professor Chen is the author or coauthor of over 1200 peer-refereed articles (over 510 in English journals) and nine books (two in English).
E-mail address: lgchenna@yahoo.com; linggenchen@hotmail.com, Fax: 0086-27-83638709 Tel: 0086-27-83615046



Fengrui Sun received his BS Degrees in 1958 in Power Engineering from the Harbing University of Technology, PR China. His work covers a diversity of topics in engineering thermodynamics, constructal theory, reliability engineering, and marine nuclear reactor engineering. He is a Professor in the Department of Power Engineering, Naval University of Engineering, PR China. He is the author or co-author of over 950 peer-refereed papers (over 440 in English) and two books (one in English).